

STRONGLY INVERTIBLE LEGENDRIAN LINKS

CARLO COLLARI AND PAOLO LISCA

ABSTRACT. We introduce and study strongly invertible Legendrian links in the standard contact three-dimensional space. We establish the equivariant analogs of basic results separately well-known for strongly invertible and Legendrian links, i.e. the existence of transversgent front diagrams, an equivariant Legendrian Reidemeister theorem, and an equivariant stabilization theorem à la Fuch-Tabachnikov. We also introduce a maximal equivariant Thurston-Bennequin number for strongly invertible links and we exhibit infinitely many such links for which the invariant coincides with the usual maximal Thurston-Bennequin number. We conjecture that such a coincidence does not hold general and that there exist strongly invertible knots having Legendrian representatives isotopic to their reversed Legendrian mirrors but not isotopic to any strongly invertible Legendrian knot.

1. INTRODUCTION

Strongly invertible knots and links have been studied for a long time [25] and they have seen a recent burst of interest [1, 3, 5, 7, 6, 8, 17, 20, 21, 22, 23, 26, 28]. On the other hand, the literature on Legendrian knots and links is quite vast and continuously expanding – we refer the reader to the surveys [12, 15]. The purpose of this paper is to initiate the study of the *strongly invertible Legendrian links* in \mathbb{R}^3 . We start by recalling the definitions of a strongly invertible link and of a Legendrian link. A link $L \subset \mathbb{R}^3$ is a finite collection of smoothly embedded circles. Let $\tau : \mathbb{R}^3 \rightarrow \mathbb{R}^3$ be the involution given by

$$\tau(x, y, z) = (x, -y, -z).$$

We say that L is *strongly invertible* if $\tau(L_i) = L_i$ for each connected component $L_i \subset L$, and $\tau|_{L_i}$ has exactly two fixed points. Two strongly invertible links are *equivalent* if there is a family of strongly invertible links that connects them. The *standard contact structure* on \mathbb{R}^3 is the tangent plane distribution $\xi_{\text{st}} := \ker(dz - ydx) \subset \mathbb{R}^3$. Note that ξ_{st} is preserved by τ . A link is *Legendrian* if it is everywhere tangent to ξ_{st} . Two Legendrian links are *equivalent* if there is a family of Legendrian links that connects them. In analogy with the above, we introduce the following definition.

Definition 1.1. *A strongly invertible Legendrian link is a link that is simultaneously strongly invertible with respect to τ and Legendrian with respect to ξ_{st} . Two strongly invertible Legendrian links are equivalent if they are connected by a smooth family of strongly invertible Legendrian links.*

Following [3], we say that a diagram D in the xz -plane is *transversgent* if the reflection map $(x, z) \mapsto (x, -z)$ fixes D setwise.

Denote by π the projection map to the xz -plane. The image $\mathcal{F} := \pi(\mathcal{L})$ of a Legendrian link \mathcal{L} is called the *front* of \mathcal{L} . It is a well-known and easy-to-show fact that, given a front \mathcal{F} , there is a unique Legendrian link \mathcal{L} such that $\pi(\mathcal{L}) = \mathcal{F}$ (see e.g. [12]). After a small, C^∞ -small Legendrian perturbation, a Legendrian link admits a generic front [27]. The diagram associated with a generic front will be called a *front diagram*. As before, we introduce the following definition in analogy to the smooth case.

Definition 1.2. *A front \mathcal{F} of a strongly invertible Legendrian link is a transversgent front if the reflection $(x, z) \mapsto (x, -z)$ fixes \mathcal{F} setwise.*

Two among the simplest examples of transversgent front diagrams are shown in Figure 1. More complicated examples are shown in Figures 25, 27, and 28.

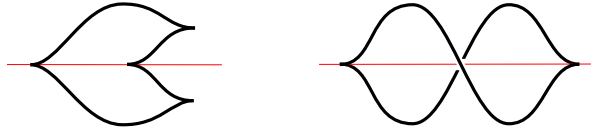


FIGURE 1. Examples of transvergent front diagrams

Recall that every strongly invertible link admits a transvergent diagram (see Section 2). Therefore, it is natural to expect that each strongly invertible link is equivalent to the strongly invertible Legendrian link associated with a transvergent front diagram. Proposition 2.2 below shows that this indeed holds.

Front diagrams of equivalent Legendrian links are connected by a sequence of Legendrian Reidemeister moves (*LR*-moves, for short) [27]. Similarly, due to a theorem of Lobb and Watson [22], transvergent diagrams of strongly invertible links (and, more generally, strongly involutive links) are connected by a sequence of equivariant moves that we call *Lobb-Watson moves* [22, Theorem 2.3]. The following is an analog for strongly invertible Legendrian links.

Theorem 1.3. *Let \mathcal{F}_0 and \mathcal{F}_1 be transvergent front diagrams of strongly invertible Legendrian links \mathcal{L}_0 and, respectively, \mathcal{L}_1 . Then, \mathcal{L}_0 and \mathcal{L}_1 are equivalent if and only if \mathcal{F}_0 and \mathcal{F}_1 are connected by a finite sequence of the following:*

- *equivariant planar isotopies;*
- *pairs of LR-moves applied symmetrically with respect to the x -axis;*
- *moves from the list of Figure 2;*
- *moves obtained from those of Figure 2 by a π -rotation of the page.*

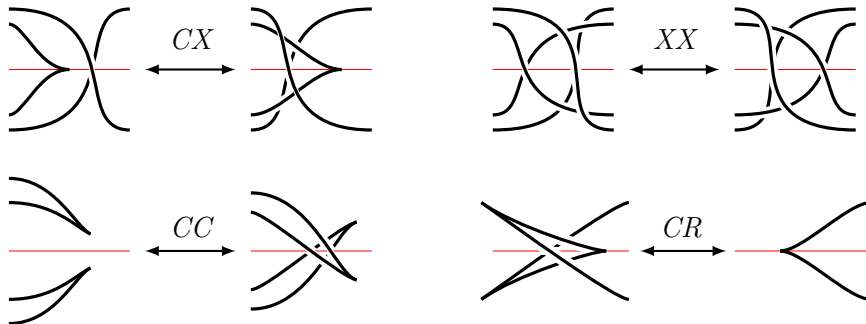
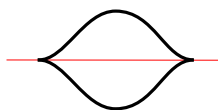


FIGURE 2. Equivariant Legendrian Reidemeister moves.

Recall that Legendrian links can be *stabilized* (see [16, §4.2] and [12, §2.7]). It is a well-known result of Fuchs and Tabachnikov that after sufficiently many stabilizations, two (oriented) Legendrian knots in $(\mathbb{R}^3, \xi_{\text{std}})$ with the same topological type become Legendrian isotopic [16, Theorem 4.4]. In Section 4 we show that an *unoriented* strongly invertible Legendrian link \mathcal{L} with the choice of a point $p = \tau(p) \in \mathcal{L}$ admits two different types of stabilizations. In particular, a strongly invertible Legendrian front \mathcal{K} with a distinguished fixed point $p \in \mathcal{K}$ admits two types of stabilizations that we call $S(\mathcal{K}, p)$ and $T(\mathcal{K}, p)$. For example, Figure 1 contains the diagrams of $\mathcal{U}_S := S(\mathcal{U}, c_R)$ (on the left) and $\mathcal{U}_T := T(\mathcal{U}, c_R)$ (on the right), where \mathcal{U} is the strongly invertible Legendrian unknot given by the diagram of Figure 3 and c_R is the fixed point corresponding to the right cusp of the diagram.

FIGURE 3. Transvergent front diagram of \mathcal{U}

The Thurston-Bennequin number is an integer-valued invariant of Legendrian knots which can

be computed directly from a front [12]. Observe that, since the Legendrian knots in Figure 1 satisfy $\text{tb}(\mathcal{U}_S) = \text{tb}(\mathcal{U}_T) = -2$, by the classification of the Legendrian unknots [11], it follows that \mathcal{U}_S and \mathcal{U}_T are Legendrian isotopic as unoriented Legendrian knots. Moreover, when the two diagrams in Figure 1 are regarded as smooth diagrams, they represent equivalent strongly invertible knots, cf. [22]. On the other hand, we show in Section 4 – see Corollary 4.6 – that the unoriented strongly invertible Legendrian unknots \mathcal{U}_S and \mathcal{U}_T are *not* equivalent.

In Section 5 we apply Theorem 1.3 to obtain the following result, which is an analog of the Fuchs and Tabachnikov’s result in the present setting.

Theorem 1.4. *Let \mathcal{L} and \mathcal{L}' be strongly invertible Legendrian links which are equivalent as strongly invertible links. Then, after sufficiently many S -stabilizations, \mathcal{L} and \mathcal{L}' become equivalent strongly invertible Legendrian links.*

Remark 1.5. To keep things simple in this paper we mainly consider strongly invertible *unoriented* Legendrian links. As in the non-equivariant case, one could introduce *oriented* strongly invertible Legendrian links and the corresponding equivalence between them. The natural analogs of Theorems 1.3 and 1.4 would still hold.

It is natural to wonder whether the maximal Thurston-Bennequin number of a strongly invertible knot is always realized by a strongly invertible Legendrian knot. This leads to the following

Definition 1.6. *Let $K \subset \mathbb{R}^3$ be a strongly invertible knot. We define the maximal equivariant Thurston-Bennequin number of K , denoted $\overline{\text{tb}}_e(K)$, as the maximal Thurston-Bennequin number of a strongly invertible Legendrian knot representing K .*

Note that the maximal equivariant Thurston-Bennequin number can be refined to yield an invariant of strongly invertible knots with a fixed involution, by considering the maximal Thurston-Bennequin number achieved within the appropriate equivalence class of strongly invertible knots. However, in this paper we do not consider such a refinement.

Denote by $\overline{\text{tb}}(K)$ the maximal Thurston-Bennequin number among all Legendrian representatives of K . For any knot K the inequality $\overline{\text{tb}}_e(K) \leq \overline{\text{tb}}(K)$ clearly holds, so it is natural to ask whether it is possible to have a strict inequality.

In Section 6 we prove the following

Proposition 1.7. *If K is either a torus knot of type $T(2, 2n+1)$, $n \in \mathbb{Z}$, or a twist knot. Then, we have $\overline{\text{tb}}_e(K) = \overline{\text{tb}}(K)$.*

On the other hand, in Section 7 we present some experimental results which suggest that the equality $\overline{\text{tb}}_e = \overline{\text{tb}}$ should not hold in general.

Remark 1.8. One may define strong invertibility with respect to the involution $\sigma : \mathbb{R}^3 \rightarrow \mathbb{R}^3$ given by $\sigma(x, y, z) = (-x, -y, z)$. Note that both the involutions τ and σ preserve ξ_{st} , but τ reverses the orientation of the contact planes, while σ preserves it. Moreover, while the fixed-point set F_τ is tangent to ξ_{std} , the fixed-point set F_σ – which coincides with the z -axis – is *transverse* to ξ_{std} . We do not investigate strong σ -invertibility in this paper.

The paper is organized as follows. In Section 2 we establish Proposition 2.2 and in Section 3 we prove Theorem 1.3. In Section 4 we define the stabilizations of strongly invertible Legendrian links and show that the strongly invertible Legendrian unknots of Figure 1 are not equivalent. In Section 5 we prove Theorem 1.4. In Section 6 we show that the equivariant maximal Thurston-Bennequin number coincides with the maximal Thurston-Bennequin number for certain families of knots. In Section 7 we describe some experimental results and state three conjectures.

Acknowledgements. The authors are grateful to Lenhard Ng for helpful e-mail messages.

2. EXISTENCE OF STRONGLY INVERTIBLE LEGENDRIAN REPRESENTATIVES

In this section, we prove Proposition 2.2. The following well-known proposition (cf. [22]) shows that, given a strongly invertible link $L \subset \mathbb{R}^3$, up to equivalence one can always assume that the

projection $\pi(L)$ on the xz -plane is generic and therefore yields a transversgent diagram of L . We include a proof for the sake of completeness and because in Section 3, we use a similar approach.

Proposition 2.1. *Each strongly invertible link L is equivalent to a strongly invertible link \tilde{L} with a transversgent diagram D . There exists D such that each crossing involves two strands meeting at a $\pi/2$ -angle, D intersects transversely the x -axis, and the restriction to D of the coordinate- x function has a finite number of critical points. Moreover, each non-crossing point of the intersection of D with the x -axis has a vertical tangent line.*

Proof. The link L can be decomposed as

$$L = A \cup \tau(A),$$

where $A \subset \mathbb{R}^3$ is a finite union of smoothly embedded arcs such that $A \cap \tau(A)$ consists of the fixed points of $\tau|_L$. By perturbing slightly A away from its endpoints, we obtain a strongly invertible link

$$\tilde{L} = \tilde{A} \cup \tau(\tilde{A})$$

which is τ -equivariantly isotopic to L , and a corresponding strongly invertible link \tilde{L} . Now, $\pi(\tilde{L})$ is generic and thus yields a transversgent diagram for L . General position ensures the stated properties of D . \square

We call “bad” a diagram crossing whose over-strand has a higher slope than the under-strand.

Proposition 2.2. *Each strongly invertible link $L \subset \mathbb{R}^3$ is equivalent to the strongly invertible Legendrian link associated with a transversgent front diagram \mathcal{F} . More precisely, given a transversgent diagram D for L , \mathcal{F} is obtained by τ -equivariantly replacing each point of D having a vertical tangent with a cusp and each “bad” crossing with either one of the configurations illustrated in Figure 4.*

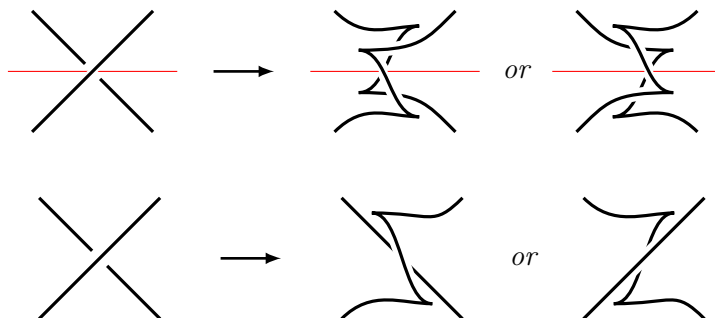


FIGURE 4. The two possible modifications near a “bad” crossing to turn a transversgent diagram into a transversgent front diagram.

Proof. Let $L \subset \mathbb{R}^3$ be a strongly invertible link and D a transversgent diagram of L as in Proposition 2.1. Arguing as in the non-equivariant case (cf. [12, Section 2.3]) we modify D into the transversgent front diagram of a strongly invertible Legendrian link equivalent to L as follows. We replace a neighborhood of each bad crossing on the x -axis with either one of the configurations at the top right of Figure 4. We replace a neighborhood of each bad crossing off the x -axis with either one of the configurations at the bottom right of Figure 4 while replacing at the same time the τ -image of the same neighborhood with the other configuration. We claim that the result of the above procedure is the transversgent front diagram of a Legendrian link equivalent to L as a strongly invertible link. Replacements of points having vertical tangents with cusps and the τ -equivariant local modifications around crossings off the x -axis do not modify the equivalence class of L as a strongly invertible link. On the other hand, it is easy to check that the local modifications around bad crossings on the x -axis amount to applications of equivariant Reidemeister moves of type M2 from Figure 9 of [22] (beware that in [22] the axis of symmetry is drawn vertically). Therefore, our claim follows from (the easy direction of) [22, Theorem 2.3] and the proof is complete. \square

We illustrate Proposition 2.2 with the following example. A transvergent diagram D of a strongly invertible unknot U is shown on the left-hand side of Figure 5. We use the procedure

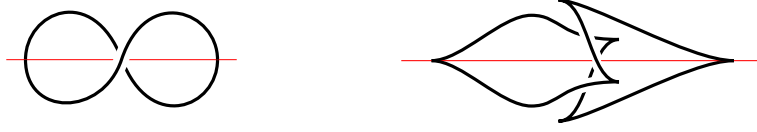


FIGURE 5. Construction of a transvergent front diagram

described in the proof of Proposition 2.2, replacing a neighborhood of the crossing on the x -axis with the rightmost picture at the top of Figure 4. The result is the transvergent front diagram \mathcal{F} shown on the right-hand side of Figure 5.

3. THE LEGENDRIAN EQUIVARIANT REIDEMEISTER THEOREM

In this section, we prove Theorem 1.3, which is an analog of the Legendrian Reidemeister theorem in the equivariant case. We also illustrate the equivariant Legendrian Reidemeister moves by show that the diagram on the right of Figure 5 and the diagram on the left of Figure 1 represent equivalent strongly invertible Legendrian unknots.

Furthermore, we describe a local modification that can be used to produce Legendrian isotopic strongly invertible Legendrian links which are equivalent as strongly invertible links, but inequivalent as strongly invertible Legendrian links.

Note that the fixed-point set F_τ of τ coincides with the x -axis, which is tangent to ξ_{std} and naturally oriented. We shall always assume F_τ to have this natural orientation.

Proof of Theorem 1.3. It is easy to see that if \mathcal{F}_0 and \mathcal{F}_1 are related by any of the moves mentioned in the statement then \mathcal{L}_0 and \mathcal{L}_1 are equivalent. Conversely, let $\{\mathcal{L}_t\}_{t \in [0,1]}$ be a family of strongly invertible Legendrian links. In general, if $t \notin \{0,1\}$ the Legendrian link \mathcal{L}_t may not have a front diagram because the front $\pi(\mathcal{L}_t)$ could be non-generic. But we claim that by applying a C^∞ -small and τ -equivariant Legendrian perturbation to the family, one can make sure that \mathcal{L}_t admits a front diagram \mathcal{F}_t for every value of t except for t belonging to a finite (possibly empty) set of “critical” values. The moves in the list of Figure 2 are obtained by comparing the fronts \mathcal{F}_t for values of t which are immediately before and after each critical value, as we now explain. We argue in a way similar to the proof of Proposition 2.1. There is a decomposition

$$\mathcal{L}_t = \mathcal{A}_t \cup \tau(\mathcal{A}_t),$$

where $\{\mathcal{A}_t\}_{t \in [0,1]}$ is a family of regular Legendrian arcs such that, for each $t \in [0,1]$, \mathcal{A}_t is a finite union of r smoothly embedded arcs such that $\mathcal{A}_t \cap \tau(\mathcal{A}_t)$ consists of the fixed points of $\tau|_{\mathcal{L}_t}$. More precisely,

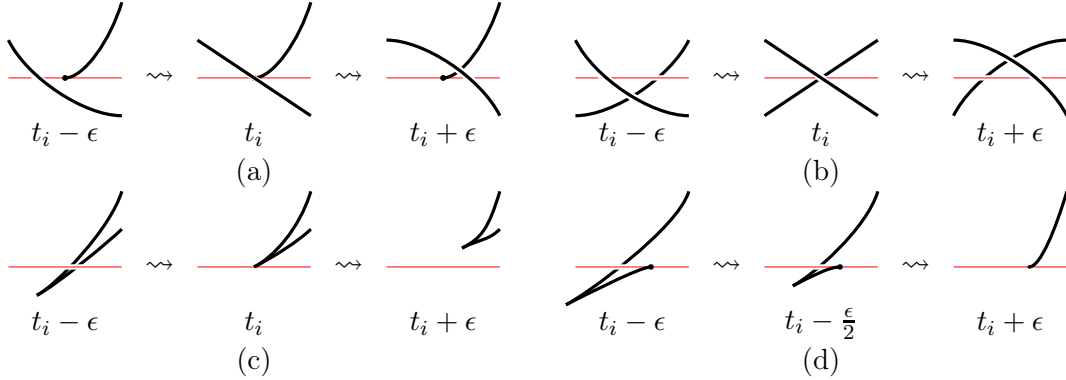
$$\partial \mathcal{A}_t = \mathcal{L}_t \cap \tau(\mathcal{L}_t) = \mathcal{L}_t \cap \{(x, 0, 0) \mid x \in \mathbb{R}\}$$

consists of $2r$ endpoints. Furthermore, the tangent line to \mathcal{A}_t at each endpoint is the direction of the y -axis.

Relative versions of the arguments in [27] imply that, after a C^∞ -small Legendrian perturbation of $\{\mathcal{A}_t\}_{t \in [0,1]}$ which coincides with the identity on the x -axis, there exists a finite subset $\{t_1, \dots, t_k\} \subset (0,1)$ such that, for each $t \notin \{t_1, \dots, t_k\}$, the front $\mathcal{F}_t = \pi(\mathcal{A}_t)$ is front diagram with no crossings nor cusps on the x -axis and such that the endpoints of \mathcal{F}_t are simple. Let us call such fronts x -generic. By general position, the projection $\pi(\mathcal{A}_t)$ can stop being an x -generic front at, say, t_i only if, as t tends towards t_i , a crossing or a cusp moves towards the x -axis or an endpoint. Given the above discussion, we may assume that, for $\varepsilon > 0$ sufficiently small, the whole front stays generic except in a small ball. Then, for each $i = 1, \dots, k$ one of the following must hold as t goes through t_i :

- (1) \mathcal{F}_t changes, away from its endpoints, as in a standard Legendrian Reidemeister move;
- (2) one strand of \mathcal{F}_t goes through some endpoint as in Figure 6(a);

- (3) one crossing of \mathcal{F}_t crosses the x -axis as in Figure 6(b);
- (4) one cusp of \mathcal{F}_t crosses the x -axis as in Figure 6(c);
- (5) one cusp reaches an endpoint and disappears as in Figure 6(d).

FIGURE 6. Examples of transitions through non- x -generic fronts.

Observe that the above requirements are equivalent to asking that the Legendrian graph given by the union of \mathcal{A}_t with the x -axis has a generic front for all but finitely many values of t , for which one of (1) – (5) happens. Now note that if $c \in \pi(\mathcal{A}_t) \setminus \{x\text{-axis}\}$ is a crossing or a cusp, by general position we may suppose that $\tau(c)$ is neither a crossing nor a cusp of $\pi(\mathcal{A}_t)$. Similarly, if $p, \tau(p) \in \pi(\mathcal{A}_t) \setminus \{x\text{-axis}\}$ and ℓ_p is the line in the xz -plane tangent to $\pi(\mathcal{A}_t)$ at p , we may assume that $\tau(\ell_p)$ is distinct from the line tangent to $\pi(\mathcal{A}_t)$ at $\tau(p)$. Under these assumptions

$$\pi(\mathcal{L}_t) = \pi(\mathcal{A}_t) \cup \pi(\tau\mathcal{A}_t)$$

is not a generic front diagram if and only if $t \in \{t_1, \dots, t_k\}$ and one of the following holds:

- \mathcal{A}_t does not have a generic front diagram and either (1) or (2) above holds;
- \mathcal{A}_t has a generic front diagram and (3), (4), or (5) above holds.

It is now straightforward to verify at each $t \in \{t_1, \dots, t_k\}$ the front $\pi(\mathcal{L}_t) = \widetilde{\mathcal{F}}_t$ changes according to one of the moves of in the statement of the theorem, so the proof is concluded. \square

Theorem 1.3 can be applied to show that the strongly invertible Legendrian unknot on the left-hand side of Figure 1 is equivalent to the strongly invertible Legendrian unknot on the right-hand side of Figure 5. Indeed, this fact follows immediately from the following more general statement.

Corollary 3.1. *Four transvergent front diagrams which differ locally as in Figure 7 represent pairwise equivalent strongly invertible Legendrian links.*

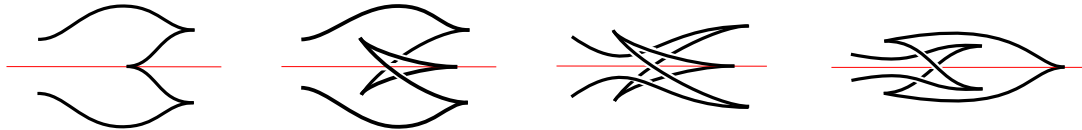


FIGURE 7. Equivalent strongly invertible Legendrian links

Proof. Denote by $\mathcal{F}_0, \mathcal{F}_1, \mathcal{F}_2$ and \mathcal{F}_3 the transvergent front diagrams differing in a disk as in Figure 7, numbered from the left to the right. Then, \mathcal{F}_1 is obtained from \mathcal{F}_0 applying a CR -move, and by a symmetric LR -move of type R2 one obtains \mathcal{F}_2 from \mathcal{F}_1 and \mathcal{F}_3 from \mathcal{F}_2 . \square

4. STABILIZATIONS OF STRONGLY INVERTIBLE LEGENDRIAN LINKS

The purpose of this section is to define stabilizations of strongly invertible Legendrian links. This will be done using transvergent front diagrams.

We will say that such a diagram is *connected* if it represents a strongly invertible knot. Similarly, given a transvergent front diagram \mathcal{F} representing a Legendrian link \mathcal{L} , we refer to the projection of each component of \mathcal{L} simply as to a *connected component* of \mathcal{F} .

The following definition introduces stabilizations for transvergent front diagrams. They will be used, in conjunction with Theorem 1.3, to define stabilizations for equivalence classes of strongly invertible Legendrian links.

Definition 4.1. Let \mathcal{F} be a connected, transvergent front diagram and $c \in \mathcal{F}$ a cusp on the x -axis. We denote by $S(\mathcal{F}, c)$ – respectively $T(\mathcal{F}, c)$ – the transvergent front diagram obtained by the operation shown in Figure 8 – respectively Figure 9. On the left-hand sides of the pictures the

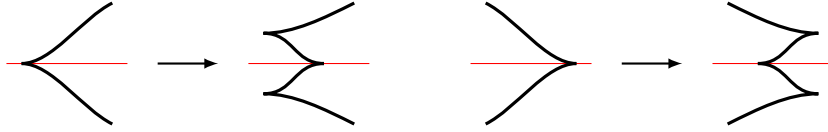


FIGURE 8. S -stabilization of a transvergent front diagram

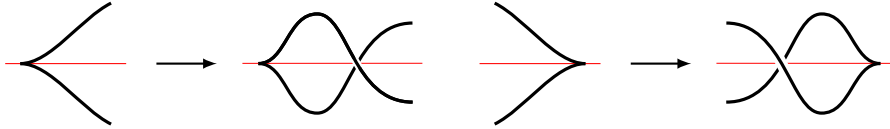


FIGURE 9. T -stabilization of a transvergent front diagram

case of a left-pointing cusp is shown, on the right-hand sides the case of a right-pointing cusp. The fronts $S(\mathcal{F}, c)$ and $T(\mathcal{F}, c)$ are, respectively, the S -stabilization and the T -stabilizations of \mathcal{F} at c .

Let \mathcal{F} be a transvergent front diagram and $c \in \mathcal{F}$ a cusp on the x -axis. We say that a cusp c is *standard* if c is a left-pointing left cusp or a right-pointing right cusp. For instance, the cusps of the diagram of Figure 3 are both standard cusps.

Definition 4.2. Let (\mathcal{L}, p) be a pair consisting of a strongly invertible Legendrian link \mathcal{L} and a distinguished point $p \in \mathcal{L}$ with $\tau(p) = p$. Given \mathcal{F} , a transvergent front diagram representing \mathcal{L} , denote by $c \in \mathcal{F}$ the cusp on the x -axis corresponding to p . The S -stabilization of \mathcal{L} at p is the strongly invertible Legendrian link $S(\mathcal{L}, p)$ determined by $S(\mathcal{F}, c)$ if c is in standard form, and by $T(\mathcal{F}, c)$ otherwise. Similarly, the T -stabilization of \mathcal{L} at p is the strongly invertible Legendrian link $T(\mathcal{L}, p)$ determined by $T(\mathcal{F}, c)$ if c is in standard form, and by $S(\mathcal{F}, c)$ otherwise.

We claim that Definition 4.2 is well-posed. Let \mathcal{F} and $M\mathcal{F}$ be two transvergent front diagrams such that $M\mathcal{F}$ is obtained from \mathcal{F} applying one of the moves M of Theorem 1.3. There is an obvious bijective correspondence between the crossings and the cusps of \mathcal{F} and $M\mathcal{F}$ outside the local picture where the two fronts differ. This correspondence can be extended to include an identification of the cusps on the axis of \mathcal{F} and $M\mathcal{F}$. We shall denote by Mc the cusp of $M\mathcal{F}$ corresponding to a cusp $c \in \mathcal{F}$ under the move M .

To check that Definition 4.2 is well-posed it will suffice to establish the following two lemmas.

Lemma 4.3. Let \mathcal{F} be a transvergent front diagram and $c \in \mathcal{F}$ a cusp on the x -axis. Suppose that $Z \in \{S, T\}$ and let M be one of the moves of Theorem 1.3 with $M \neq CR$. Then, the diagrams $Z(M\mathcal{F}, Mc)$ and $Z(\mathcal{F}, c)$ represent equivalent strongly invertible links.

Proof. When $M \in \{XX, CC, SR\}$ the statement is clear because M and Z are supported on disjoint discs. The same holds if $M = CX$ but it involves a cusp different from c . If $M = CX$ involves the cusp c and $Z = S$, then $Z(\mathcal{F}, c)$ is obtained from $Z(M\mathcal{F}, Mc)$ by applying one CX -move and two symmetric Reidemeister moves, see Figure 10 for an exemplification. Similarly, if

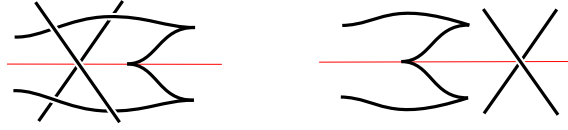


FIGURE 10. The transvergent front diagrams $Z(M\mathcal{F}, Mc)$ (left) and $Z(\mathcal{F}, c)$ (right) for $M = CX$ and $Z = S$

$Z = T$, then $Z(\mathcal{F}, c)$ is obtained from $Z(M\mathcal{F}, Mc)$ by applying one CX -move and one XX -move, see Figure 11. Figures 10 and 11 illustrate the cases when c is a right-pointing cusp. The



FIGURE 11. The transvergent front diagrams $Z(M\mathcal{F}, Mc)$ (left) and $Z(\mathcal{F}, c)$ (right) for $M = CX$ and $Z = T$

cases when c is left-pointing are completely analogous, and the corresponding equivalence can be obtained from those in Figures 10 and 11 by a π rotation of the plane. \square

Given $Z \in \{S, T\}$, we denote by \overline{Z} the operation obtained from Z by swapping the letters S and T , so that $\overline{S} = T$ and $\overline{T} = S$.

Lemma 4.4. *Let \mathcal{F} be a transvergent front diagram, $c \in \mathcal{F}$ a cusp on the x -axis, and let $Z \in \{S, T\}$. Then, the diagrams $Z(CR\mathcal{F}, CRc)$ and $\overline{Z}(\mathcal{F}, c)$ represent equivalent strongly invertible links.*

Proof. When c is right-pointing, Figure 12 shows that $S(CR\mathcal{F}, CRc)$ and $T(\mathcal{F}, c)$ are obtained from each other by a CX move, a symmetric $R2$ -move and a symmetric $R1$ -move. Similarly,

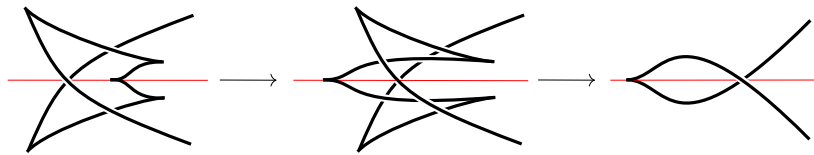


FIGURE 12. Equivalence of $S_R(CR\mathcal{F}, CRc)$ and $T(\mathcal{F}, c)$.

Figure 13 shows that $T(CR\mathcal{F}, CRc)$ and $S(\mathcal{F}, c)$ are obtained from each other by a CC move. When c is left-pointing the argument is similar. The corresponding diagrams are obtained from

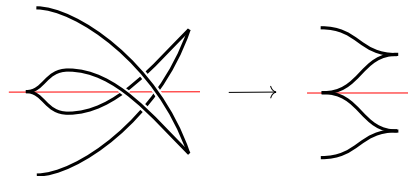


FIGURE 13. Equivalence between $T(CR\mathcal{F}, CRc)$ and $S(\mathcal{F}, c)$.

those of Figures 12 and 13 by a π -rotation. \square

Proposition 4.5. *Definition 4.2 is well-posed.*

Proof. Suppose that (\mathcal{F}, c) and (\mathcal{F}', c') are transvergent front diagrams with distinguished cusps on the x -axis. Then, (\mathcal{F}, c) and (\mathcal{F}', c') are connected by a sequence $\{M_i\}_{i=0}^k$ of the moves of Theorem 1.3. In other words, there is a sequence (\mathcal{F}_i, c_i) , $i = 0, \dots, k$, of transvergent front diagrams with distinguished cusps on the x -axis such that $(\mathcal{F}_0, c_0) = (\mathcal{F}, c)$, $(\mathcal{F}_k, c_k) = (\mathcal{F}', c')$ and $(\mathcal{F}_{i+1}, c_{i+1}) = (M_i \mathcal{F}_i, M_i c_i)$ for each $i = 0, \dots, k$. Assume first that either both c and c' are in standard form or neither of them is. We need to check that, for any $Z \in \{S, T\}$, the strongly invertible Legendrian link given by $Z(\mathcal{F}, c)$ is equivalent to the strongly invertible Legendrian link given by $Z(\mathcal{F}', c')$. Since c is in standard form if and only if so is c' , the total number of CR moves among the M_i 's must be even. Using this together with the fact that the transformation $Z \rightarrow \overline{Z}$ is an involution and applying Lemmas 4.3 and 4.4, we conclude that $Z(\mathcal{F}, c)$ and $Z(\mathcal{F}', c')$ are equivalent. Now suppose that exactly one among c and c' is in standard form. In this case we have to check that the strongly invertible Legendrian link given by $Z(\mathcal{F}, c)$ is equivalent to the strongly invertible Legendrian link given by $\overline{Z}(\mathcal{F}', c')$. Moreover, the total number of CR moves among the M_i 's is odd. The conclusion follows from Lemmas 4.3 and 4.4 as in the previous case. \square

With Definition 4.2 in place, we can now observe that the strongly invertible Legendrian unknots given in Figure 1 are nothing but $S(\mathcal{U}, c_R)$ and $T(\mathcal{U}, c_R)$, where \mathcal{U} is given by the diagram of Figure 3 and c_R is the fixed point corresponding to the right cusp. As we observed in Section 1, the Thurston-Bennequin numbers of $\mathcal{U}_S := S(\mathcal{U}, c_R)$ and $\mathcal{U}_T := T(\mathcal{U}, c_R)$ are both equal to -2 . Thus, by the classification of Legendrian unknots [11], \mathcal{U}_S and \mathcal{U}_T are equivalent as unoriented Legendrian knots. On the other hand, the following corollary of Theorem 1.3 implies that \mathcal{U}_S and \mathcal{U}_T are not equivalent as strongly invertible Legendrian knots.

Corollary 4.6. *Two transvergent front diagrams which differ only in a disk as in Figure 14 represent strongly invertible Legendrian links not equivalent to each other. In particular, if (\mathcal{K}, p)*

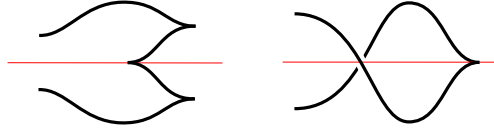


FIGURE 14. Not equivalent strongly invertible Legendrian links

is a strongly invertible Legendrian knot with a distinguished fixed point $p \in \mathcal{K}$, then $S(\mathcal{K}, p)$ and $T(\mathcal{K}, p)$ are not equivalent.

Proof. Let \mathcal{F} and \mathcal{F}' the transvergent front diagrams differing only in a disk as in Figure 14. Suppose by contradiction that the corresponding strongly invertible links \mathcal{L} and \mathcal{L}' are equivalent. Then, the fronts \mathcal{F} and \mathcal{F}' should be connected by a sequence of moves as in Theorem 1.3. Fix an orientation \mathcal{O} on \mathcal{F} which makes the relevant cusp point upwards. Then, a moment's reflection shows that the moves of Theorem 1.3 carry \mathcal{O} to an orientation of \mathcal{F}' which makes the corresponding cusp point upwards. But a simple calculation shows that, denoting by $\vec{\mathcal{L}}$ and $\vec{\mathcal{L}}'$, respectively, the oriented versions of \mathcal{L} and \mathcal{L}' , their rotation numbers satisfy $\text{rot}(\vec{\mathcal{L}}) - \text{rot}(\vec{\mathcal{L}}') = 2$, contradicting the fact that the rotation number is invariant under oriented Legendrian isotopy [12]. Therefore \mathcal{L} and \mathcal{L}' are not equivalent. To prove the last part of the statement, let (\mathcal{F}, c) be a transvergent front diagram of \mathcal{K} with distinguished cusp $c \in \mathcal{F}$ corresponding to the fixed point p . When c is right-pointing, the conclusion follows immediately by applying the argument above in a neighborhood of c . When c is left-pointing, the conclusion is obtained using the same argument to the pictures of Figure 14 rotated by π . \square

5. THE PROOF OF THEOREM 1.4

Up to equivalence, we may assume that $\mathcal{L}_0 := \mathcal{L}$ and $\mathcal{L}_1 := \mathcal{L}'$ have transvergent front diagrams in standard form \mathcal{F}_0 and \mathcal{F}_1 . We can turn \mathcal{F}_i , $i = 0, 1$, into a transvergent diagram

D_i by smoothing all cusps. Let L_0 and L_1 be the strongly invertible links such that $\pi(L_i) = D_i$, $i = 0, 1$. By assumption, there exists a smooth, equivariant isotopy L_t , $t \in [0, 1]$ from L_0 to L_1 . Our argument will be an adaptation of the argument from [16, Theorem 4.4]. Call a value of t *generic* if (i) the projection $\pi(L_t)$ is regular, (ii) its self-intersections are transverse double points, (iii) neither tangent line at each self-intersection point is vertical and (iv) no tangent line at an inflection point is vertical. When t is generic, the projection $\pi(L_t)$ is a transversent diagram of L_t and we denote it by D_t . By general position, we may assume that there are finitely many non-generic values, say $t_1, \dots, t_k \in (0, 1)$, that we call the *singular values*. By the Lobb-Watson equivariant Reidemeister theorem [22, Theorem 2.3], for some small $\varepsilon > 0$ and each singular value t_i , the diagrams $D_{t_i-\varepsilon}$ and $D_{t_i+\varepsilon}$ differ by one of the equivariant Reidemeister moves given in [22, Figure 9] or by equivariant planar isotopy. We warn the reader that Lobb and Watson draw their pictures using a vertical axis of symmetry, while we always represent the x -axis as horizontal. In the notation of [22, Figure 9], (i) is violated if and only if $D_{t_i-\varepsilon}$ and $D_{t_i+\varepsilon}$ differ by a move of type IR1 or R1, (ii) is violated if and only if $D_{t_i-\varepsilon}$ and $D_{t_i+\varepsilon}$ differ by one of the remaining equivariant Reidemeister moves and (iii), (iv) are violated during equivariant planar isotopies. We can apply Proposition 2.2 to “Legendrianize” D_0 and D_1 and obtain precisely the transversent front diagrams in standard form \mathcal{F}_0 and \mathcal{F}_1 . Since each $t \in [0, t_1 - \varepsilon]$ is regular, the whole family D_t , $t \in [0, t_1 - \varepsilon]$, can be Legendrianized, therefore the front \mathcal{F}_0 extends to a family of transversent front diagrams \mathcal{F}_t which lift to strongly invertible Legendrian links \mathcal{L}_t for $t \in [0, t_1 - \varepsilon]$. This argument applies, more generally, to D_t for

$$t \in A := [0, t_1 - \varepsilon] \cup [t_1 + \varepsilon, t_2 - \varepsilon] \cup \dots \cup [t_k + \varepsilon, 1] \subset [0, 1],$$

yielding strongly invertible Legendrian links \mathcal{L}_t with transversent front diagrams \mathcal{F}_t .

Observe that after a number of S -stabilizations we can create arbitrarily many symmetric pairs of “zig-zags” on the fronts \mathcal{F}_t – cf. [12, Figure 19] for the definition of “zig-zag” in the non-equivariant setting. Moreover, using the moves of Theorem 1.3 we can equivariantly relocate any symmetric pair of “zag-zags” to an arbitrarily chosen place. This follows simply by “symmetrizing” the proof of [16, Lemma 4.3] as long as the new positions of the symmetric “zag-zags” can be reached by moving along arcs of the diagram without crossing the axis. To deal with the case when the “zig-zags” need to cross the axis, we are going to show that two transversent fronts differing as in Figure 15 represent equivalent strongly invertible links. An analogous



FIGURE 15. Symmetric “zig-zags” can be moved across the x -axis

statement holds for the other type of “zig-zag”. The equivalence of the two links is illustrated in Figure 16, where the first diagram from the left (right, respectively) is obtained from the left (right, respectively) diagram of Figure 15 by a symmetric $R2$ -move. The proof for the other type

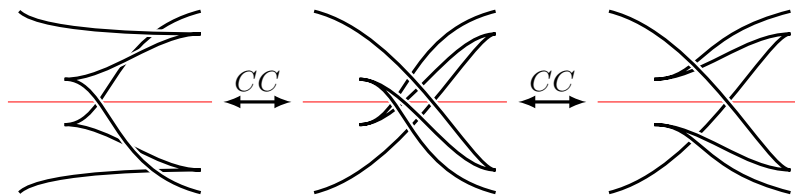


FIGURE 16. Equivalence of stabilizations

of zig-zag is similar and left to the reader.

We now claim that, for each $i = 1, \dots, k$ the strongly invertible Legendrian knots $\mathcal{L}_{t_i-\varepsilon}$ and $\mathcal{L}_{t_i+\varepsilon}$ become equivalent after applying sufficiently many S -stabilizations. If $D_{t_i-\varepsilon}$ and $D_{t_i+\varepsilon}$ differ by one of the moves IR1, IR2 or IR3 the claim follows by “symmetrizing” and possibly slightly adapting Pictures R1(a), R2(a) and R3 of [16, Figure 22]. Note that in such adaptations one needs to take into account the choice of configuration in Figure 4 made to Legendrianize $D_{t_i+\varepsilon}$. If either condition (iii) or condition (iv) is violated at a point of D_{t_i} away from the x -axis, we need to “symmetrize” the stabilizations provided in the proof of [16, Theorem 4.4] – specifically, those of Pictures V1, V2 in [16, Figure 21] and Pictures V1(a), V2(a) in [16, Figure 22].

It remains to deal with the cases when one of the conditions (i)–(iv) is violated at a point of D_{t_i} lying on the x -axis. We deal first with the violation of (i) or (ii) on the x -axis, in which cases $D_{t_i-\varepsilon}$ and $D_{t_i+\varepsilon}$ differ by a Lobb-Watson move of type $R1$, $R2$, $M1$, $M2$ or $M3$. Therefore, we may assume that $\mathcal{F}_{t_i-\varepsilon}$ and $\mathcal{F}_{t_i+\varepsilon}$ differ by a “Legendrianization” of one of the five moves. For each of the five moves, we need to show that, after sufficiently many equivariant stabilizations, $\mathcal{F}_{t_i-\varepsilon}$ and $\mathcal{F}_{t_i+\varepsilon}$ differ by a sequence of moves from the list of Theorem 1.3.

move R1: Up to a π -rotation of the page, the transvergent front diagram $\mathcal{F}_{t_i-\varepsilon}$ is given, in a disk, by the first picture from the left of Figure 17. There are two possible cases for the front

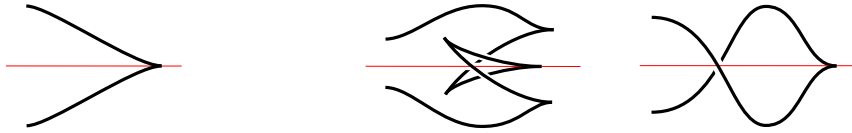


FIGURE 17. $R1$: transvergent fronts $\mathcal{F}_{t_i-\varepsilon}$ and $\mathcal{F}_{t_i+\varepsilon}$ (both types of crossing)

diagram $\mathcal{F}_{t_i+\varepsilon}$, depending on the type of crossing in the move. When the crossing is positive, $\mathcal{F}_{t_i+\varepsilon}$ appears as in the central picture of Figure 17, and it is obtained from an equivariant stabilization of $\mathcal{F}_{t_i-\varepsilon}$ by a CR -move. When the crossing is negative, $\mathcal{F}_{t_i+\varepsilon}$ appears as the first picture from the right of Figure 17. In this case, a sequence of moves connecting suitable equivariant stabilizations of $\mathcal{F}_{t_i-\varepsilon}$ and $\mathcal{F}_{t_i+\varepsilon}$ can be obtained using the fronts shown in Figure 18. More precisely, the leftmost front in Figure 18 is obtained from $\mathcal{F}_{t_i-\varepsilon}$ by performing a CR -move

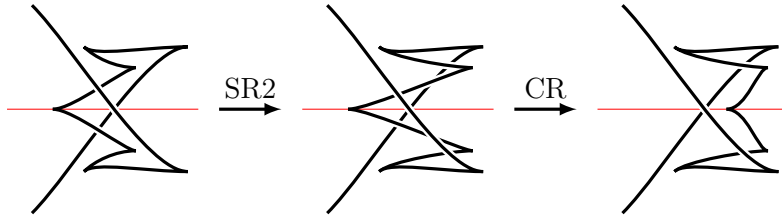


FIGURE 18. $R1$: equivalence of $\mathcal{F}_{t_i-\varepsilon}$ and $\mathcal{F}_{t_i+\varepsilon}$ up to stabilizations

and two equivariant stabilizations, while by performing two symmetric $R1$ on the rightmost front one obtains a stabilization of $\mathcal{F}_{t_i+\varepsilon}$.

move R2: Up to π -rotation, there are two types of $R2$ -moves, but they can be treated similarly, so without loss of generality we fix an arbitrary choice. The corresponding fronts $\mathcal{F}_{t_i-\varepsilon}$ and $\mathcal{F}_{t_i+\varepsilon}$ are given in Figure 19. The equivalence of $\mathcal{F}_{t_i-\varepsilon}$ and $\mathcal{F}_{t_i+\varepsilon}$ up to equivariant stabilizations is

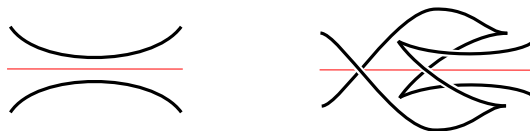
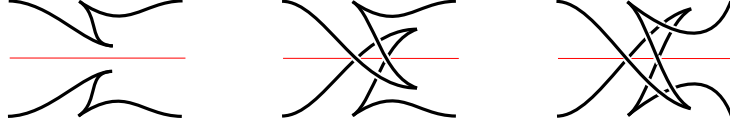


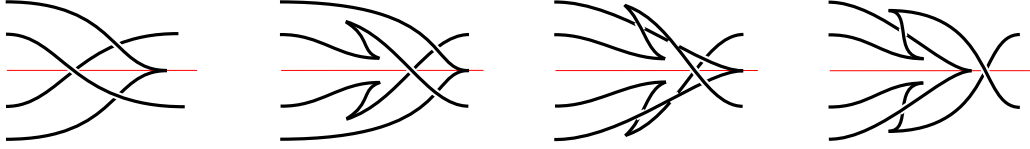
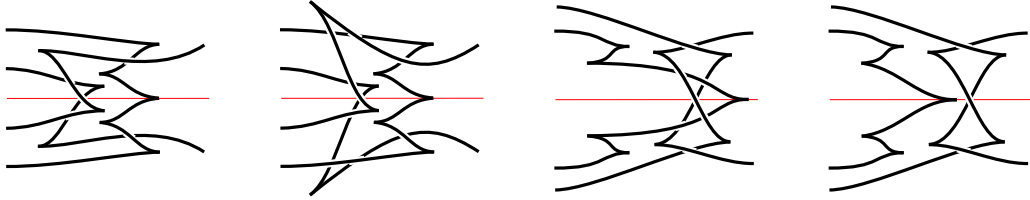
FIGURE 19. $R2$: the fronts $\mathcal{F}_{t_i-\varepsilon}$ and $\mathcal{F}_{t_i+\varepsilon}$

illustrated in Figure 20. Indeed, the pictures show that applying to $\mathcal{F}_{t_i-\varepsilon}$ one equivariant

FIGURE 20. $R2$: equivalence of $\mathcal{F}_{t_i-\varepsilon}$ and $\mathcal{F}_{t_i+\varepsilon}$ up to stabilizations

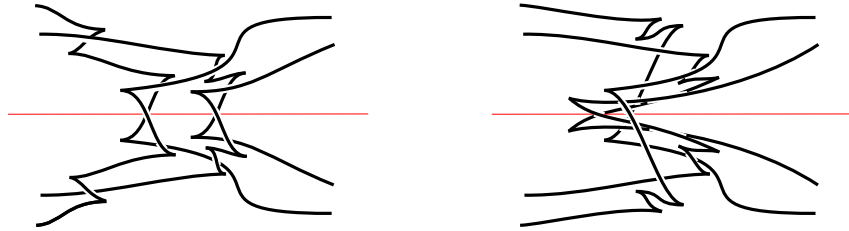
stabilization, a CC -move, and a symmetric LR -move, the resulting front is obtained from $\mathcal{F}_{t_i+\varepsilon}$ by another symmetric LR -move.

move M1: Up to rotation, there are two cases, depending on the type of crossing on the x -axis. In the first case, the equivalence of $\mathcal{F}_{t_i-\varepsilon}$ and $\mathcal{F}_{t_i+\varepsilon}$ up to stabilizations is shown in Figure 21. In the second case, the equivalence is shown in Figure 22.

FIGURE 21. $M1$ (first case): equivalence of $\mathcal{F}_{t_i-\varepsilon}$ and $\mathcal{F}_{t_i+\varepsilon}$ up to stabilizationsFIGURE 22. $M1$ (second case): equivalence of $\mathcal{F}_{t_i-\varepsilon}$ and $\mathcal{F}_{t_i+\varepsilon}$ up to stabilizations

move M2: Again, there are two cases up to rotation, depending on the crossing on the x -axis. But in one case $\mathcal{F}_{t_i-\varepsilon}$ and $\mathcal{F}_{t_i+\varepsilon}$ are identical, so there is nothing to prove. In the other case, it is immediately evident that $\mathcal{F}_{t_i-\varepsilon}$ is obtained directly from $\mathcal{F}_{t_i+\varepsilon}$ by equivariant stabilization. We omit the obvious pictures.

move M3: There are several cases depending on the types of crossings. They can all be treated in similar ways, so we just show how to deal with the most complicated case – see Figures 23 and 24.

FIGURE 23. $M3$: equivalence of $\mathcal{F}_{t_i-\varepsilon}$ and $\mathcal{F}_{t_i+\varepsilon}$ up to stabilizations (first part)

We can now assume that (i) and (ii) hold. Then, neither (iii) nor (iv) can be violated at a point of D_{t_i} on the x -axis, because equivariance would imply that both tangent lines are vertical, which contradicts (ii). This concludes the proof of Theorem 1.4. \square

6. REALIZATION OF MAXIMAL EQUIVARIANT THURSTON-BENNEQUIN NUMBERS

In this section we exhibit two infinite families of strongly invertible Legendrian links which maximize the equivariant Thurston-Bennequin number.

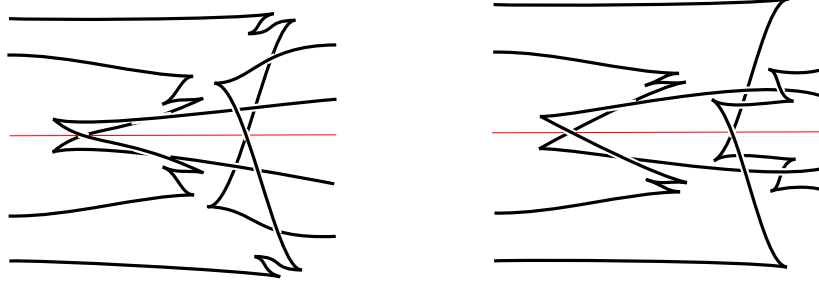


FIGURE 24. $M3$: equivalence of $\mathcal{F}_{t_i - \epsilon}$ and $\mathcal{F}_{t_i + \epsilon}$ up to stabilizations (second part)

Proof of Proposition 1.7. The maximal Thurston-Bennequin number of torus knots was computed in [13, Theorem 4.1]:

$$\overline{\text{tb}}(T(2, 2n + 1)) = \begin{cases} 2n - 1 & n \geq 0, \\ 4n - 2 & n < 0. \end{cases}$$

Strongly invertible Legendrian representatives realizing the maximal Thurston-Bennequin number for $T(2, 2n + 1)$ are shown in Figure 25.

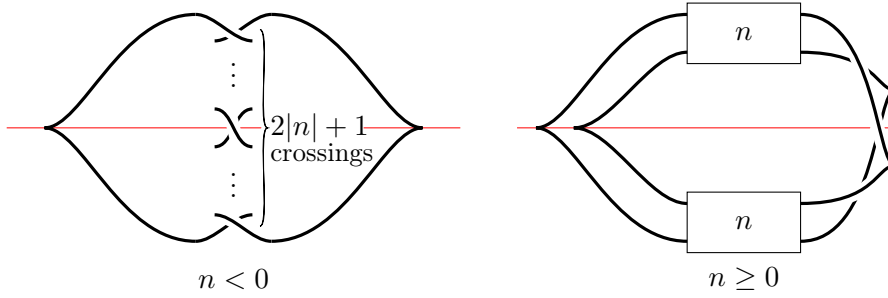


FIGURE 25. Strongly invertible Legendrian representatives of $T(2, 2n + 1)$ for each n . Each box contains n right-handed half twists.

Denote by K_m the twist knot of Figure 26. It was proved in [14, Proposition 2.6] that

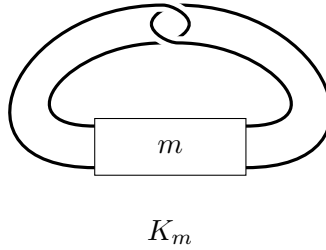


FIGURE 26. The twist knot K_m . The box contains m right-handed half twists if $m \geq 0$, and $|m|$ left-handed half twists if $m < 0$.

$$\overline{\text{tb}}(K_m) = \begin{cases} -m - 1 & m \geq 0 \text{ and even,} \\ -m - 5 & m \geq 0 \text{ and odd,} \\ -1 & m = -1, \\ 1 & m < 0 \text{ and even,} \\ -3 & m < -1 \text{ and odd.} \end{cases}$$

Note that K_{-1} and K_0 are both the unknot, and the desired strongly invertible Legendrian representative is shown in Figure 3. In the remaining cases, the strongly invertible Legendrian representatives are shown in Figure 27. This proves the statement for twist knots. \square

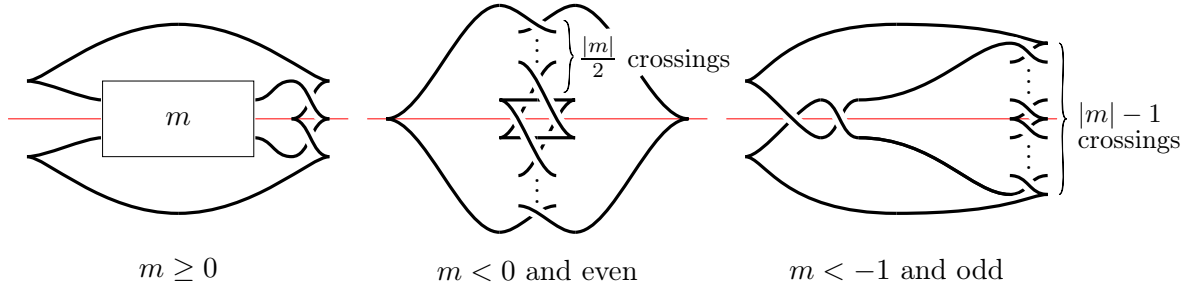


FIGURE 27. Strongly invertible Legendrian representatives of maximal Thurston Bennequin number for K_m , with $m \neq -1$.

7. EXPERIMENTAL RESULTS AND CONJECTURES

In this section we discuss some experimental results and state three conjectures.

In view of Proposition 1.7, we looked for strongly invertible Legendrian knots realizing the maximal Thurston-Bennequin number in the simplest strongly invertible knot types which are neither twist knots nor of type $T(2, 2n + 1)$. Among the knots appearing in [4], which have grid number less than 10, we could find such Legendrian representatives up to and including crossing number eight. On the other hand, we were unable to find strongly invertible Legendrian representatives for each knot type with grid number less than ten and crossing number nine. For example, according to [4] we have $\overline{\text{tb}}(9_{42}) = -3$, but we could not find a strongly invertible Legendrian knot of type 9_{42} with Thurston-Bennequin number bigger than -5 .

On the basis of our experimental evidence we formulate the following

Conjecture 7.1. $\overline{\text{tb}}_e(9_{42}) < \overline{\text{tb}}(9_{42})$.

Recall that, given an oriented Legendrian knot $\vec{\mathcal{K}} \subset \mathbb{R}^3$, the *Legendrian mirror* $\mu(\vec{\mathcal{K}})$ is obtained from $\vec{\mathcal{K}}$ by a π -rotation around the x -axis [12]. It is easy to check that, for any choice of orientation, a strongly invertible Legendrian knot coincides with its reversed Legendrian mirror. The oriented Legendrian representative of 9_{42} with maximal Thurston-Bennequin number shown in [4] is not isotopic to its reversed Legendrian mirror, so we initially wondered whether this phenomenon could be the only one obstructing the equality $\overline{\text{tb}}_e = \overline{\text{tb}}$. Then, we became aware of the knot type $m(10_{125})$, denoted by $m10n2$ in [24], for which every maximal Legendrian representative listed in [24] is equivalent to its reversed Legendrian mirror. We were unable to find a strongly invertible representative of $m(10_{125})$ with maximal Thurston-Bennequin invariant. Hence, we state the following:

Conjecture 7.2. *Let \mathcal{K} be a Legendrian knot representing $m(10_{125})$ with $\text{tb}(\mathcal{K}) = -6$. Then, \mathcal{K} is Legendrian isotopic to $-\mu(\mathcal{K})$ but not to a strongly invertible Legendrian knot.*

Recall that the Jones' conjecture proved in [10, 19] implies the equality

$$(1) \quad \overline{\text{tb}}(K) + \overline{\text{tb}}(m(K)) = -\text{grid number}(K) .$$

One can introduce a natural definition of “equivariant grid number” for a strongly invertible knot, as the minimal grid number of a symmetric grid (with respect to the north-west-to-south-east diagonal) realizing the given knot type. A positive answer to Conjecture 7.2 would yield a counterexample to the equivariant analog of Equation (1), where $\overline{\text{tb}}$ is replaced with $\overline{\text{tb}}_e$ and the grid number with the equivariant grid number. In fact, this conclusion would follow from the fact, which we have verified, that both the grid number and the Thurston-Bennequin number of the knot type 10_{125} coincide with their equivariant analogs.

Aside from the equality $\overline{\text{tb}}_e = \overline{\text{tb}}$, one could investigate the existence of strongly invertible oriented Legendrian knots with a given pair of values (tb, rot) . For example, according to [24] there is an oriented Legendrian knot $\overrightarrow{\mathcal{K}}$ of type 8_5 , Legendrian isotopic to $-\mu(\overrightarrow{\mathcal{K}})$, with $\text{tb}(\overrightarrow{\mathcal{K}}) = -11$ and $\text{rot}(\overrightarrow{\mathcal{K}}) = 2$. We could find a strongly invertible oriented Legendrian representative of 8_5 with $(\text{tb}, \text{rot}) = (-11, 0)$, but were unable to find a strongly invertible Legendrian knot isotopic to \mathcal{K} with either orientation. As a result, we state the following:

Conjecture 7.3. *Let $\overrightarrow{\mathcal{K}}$ be a strongly invertible oriented Legendrian knot of type 8_5 with $\text{tb}(\overrightarrow{\mathcal{K}}) = -11$. Then, $\text{rot}(\overrightarrow{\mathcal{K}}) = 0$.*

We close the paper with the description of a fortuitous discovery. While examining nine-crossing knots we ran into the following example, which shows that the information in [4] about $m(9_{44})$ needs to be slightly revised. Consider the oriented Legendrian knot $\overrightarrow{\mathcal{K}}_1$ with topological type $m(9_{44})$ and maximal Thurston-Bennequin number -3 described in [4], where one finds the claim that $\overrightarrow{\mathcal{K}}_1$ is Legendrian isotopic to its Legendrian mirror¹. We were unable to verify the claim using *KnotMatcher* [2]. In fact, we are going to show that the claim leads to a contradiction with recent work of Dynnikov and Shastin [9]. Let \mathcal{K}_1 be the unoriented Legendrian knot underlying $\overrightarrow{\mathcal{K}}_1$. A front diagram for \mathcal{K}_1 is illustrated on the left of Figure 28. It can be verified

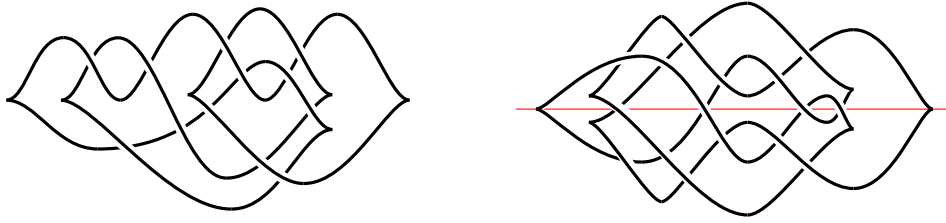


FIGURE 28. The two Legendrian knots \mathcal{K}_1 (left) and \mathcal{K}_2 (right)

using *KnotMatcher* that \mathcal{K}_1 is Legendrian isotopic to the strongly invertible Legendrian knot \mathcal{K}_2 with transvergent front diagram shown on the right of Figure 28. Thus, we can choose an orientated version $\overrightarrow{\mathcal{K}}_2$ of \mathcal{K}_2 Legendrian isotopic to $\overrightarrow{\mathcal{K}}_1$. Therefore we have $\overrightarrow{\mathcal{K}}_1 = \overrightarrow{\mathcal{K}}_2 = -\mu(\overrightarrow{\mathcal{K}}_2) = -\mu(\overrightarrow{\mathcal{K}}_1)$. But by [9, Proposition 7.4] the Legendrian knot $\overrightarrow{\mathcal{K}}_1$ is not isotopic to its reverse $-\overrightarrow{\mathcal{K}}_1$. This implies that $\overrightarrow{\mathcal{K}}_1$ is not Legendrian isotopic to $\mu(\overrightarrow{\mathcal{K}}_1)$, contrary to the claim made in [4]. Summarizing, the previous considerations show that the entry for $m(9_{44})$ in [4] should be amended as follows:

| Knot | Grid | (tb, r) | $L = -L?$ | $L = \mu(L)?$ | $L = -\mu(L)?$ | Ruling polynomial | LCH |
|-------------|------|------------------|-----------|---------------|----------------|-------------------|---------------|
| $m(9_{44})$ | | $(-3, 0)$ | \times | \times | \checkmark | 1 | $t^{-1} + 2t$ |

REFERENCES

- [1] A. Alfieri and K. Boyle. “Strongly invertible knots, invariant surfaces, and the Atiyah-Singer signature theorem”. In: *arXiv preprint arXiv:2109.09915* (2021).
- [2] M. An, E. Liang, and A. Manocha. *KnotMatcher*. available at <https://services.math.duke.edu/~ng/atlas/>.

¹In [4] the Legendrian mirror is defined using π -rotation around the y -axis, but this definition yields an equivalent Legendrian to the one above. This follows from [18, Theorem 1.2] and the fact that the composition of the two rotations is a contactomorphism which preserves the orientation of the contact planes.

- [3] K. Boyle and A. Issa. “Equivariant 4-genera of strongly invertible and periodic knots”. In: *J. Topol.* 15.3 (2022), pp. 1635–1674. DOI: <https://doi.org/10.1112/topo.12254>.
- [4] W. Chongchitmate and L. Ng. “An atlas of Legendrian knots”. In: *Exp. Math.* 22.1 (2013), pp. 26–37. URL: <https://doi.org/10.1080/10586458.2013.750221>.
- [5] I. Dai, A. Mallick, and M. Stoffregen. “Equivariant knots and knot Floer homology”. In: *Journal of Topology* 16.3 (2023), pp. 1167–1236. URL: <https://doi.org/10.1112/topo.12312>.
- [6] A. Di Prisa. “Equivariant algebraic concordance of strongly invertible knots”. In: *arXiv preprint arXiv:2303.11895* (2023).
- [7] A. Di Prisa. “The equivariant concordance group is not abelian”. In: *Bulletin of the London Mathematical Society* 55.1 (2023), pp. 502–507. URL: <https://doi.org/10.1112/blms.12741>.
- [8] A. Di Prisa and G. Framba. “A new invariant of equivariant concordance and results on 2-bridge knots”. In: *arXiv preprint arXiv:2303.08794* (2023).
- [9] I. Dynnikov and V. Shastin. “Distinguishing Legendrian knots with trivial orientation-preserving symmetry group”. In: *Algebr. Geom. Topol.* 23 (2023). URL: <https://doi.org/10.2140/agt.2023.23.1849>.
- [10] I. A. Dynnikov and M. V. Prasolov. “Bypasses for rectangular diagrams. A proof of the Jones conjecture and related questions”. In: *Trans. Moscow Math. Soc.* (2013), pp. 97–144. URL: <https://doi.org/10.1090/s0077-1554-2014-00210-7>.
- [11] Y. Eliashberg and M. Fraser. “Topologically trivial Legendrian knots”. In: *J. Symplectic Geom.* 7.2 (2009), pp. 77–127. URL: <http://dml.mathdoc.fr/item/1239974381>.
- [12] J. B. Etnyre. “Legendrian and transversal knots”. In: *Handbook of knot theory*. Elsevier, 2005, pp. 105–185.
- [13] J. B. Etnyre and K. Honda. “Knots and contact geometry. I. Torus knots and the figure eight knot”. In: *J. Symplectic Geom.* 1.1 (2001), pp. 63–120. URL: <http://projecteuclid.org/euclid.jsg/1092316299>.
- [14] J. B. Etnyre, L. Ng, and V. Vértési. “Legendrian and transverse twist knots”. In: *J. Eur. Math. Soc. (JEMS)* 15.3 (2013), pp. 969–995. URL: <https://doi.org/10.4171/JEMS/383>.
- [15] J. B. Etnyre and L. L. Ng. “Legendrian contact homology in \mathbb{R}^3 ”. In: *Surveys in differential geometry* 25.1 (2020).
- [16] D. Fuchs and S. Tabachnikov. “Invariants of Legendrian and transverse knots in the standard contact space”. In: *Topology* 36.5 (1997), pp. 1025–1053. URL: [https://doi.org/10.1016/S0040-9383\(96\)00035-3](https://doi.org/10.1016/S0040-9383(96)00035-3).
- [17] M. Hirasawa, R. Hiura, and M. Sakuma. “Invariant Seifert surfaces for strongly invertible knots”. In: *arXiv preprint arXiv:2206.02097* (2022).
- [18] M. Kegel. “The Legendrian knot complement problem”. In: *J. Knot Theory Ramifications* 27.14 (2018), pp. 1850067, 36. URL: <https://doi.org/10.1142/S0218216518500670>.
- [19] D. J. LaFountain and W. W. Menasco. “Embedded annuli and Jones’ conjecture”. In: *Algebr. Geom. Topol.* 14.6 (2014), pp. 3589–3601. URL: <https://doi.org/10.2140/agt.2014.14.3589>.
- [20] C. Lamm. “Symmetric diagrams for all strongly invertible knots up to 10 crossings”. In: *arXiv preprint arXiv:2210.13198* (2022).
- [21] R. Lipshitz and S. Sarkar. “Khovanov homology of strongly invertible knots and their quotients”. In: *arXiv preprint arXiv:2203.13895* (2022).
- [22] A. Lobb and L. Watson. “A refinement of Khovanov homology”. In: *Geom. Topol.* 25.4 (2021), pp. 1861–1917. URL: <https://doi.org/10.2140/gt.2021.25.1861>.
- [23] A.N. Miller and M. Powell. “Strongly invertible knots, equivariant slice genera, and an equivariant algebraic concordance group”. In: *Journal of the London Mathematical Society* 107 (2023), pp. 2025–2053. URL: <https://doi.org/10.1112/jlms.12732>.
- [24] I. Petkova and N. Schwartz. “A Legendrian knot atlas for knots of arc index 10”. In: *arXiv preprint arXiv:2307.11212* (2023).
- [25] M. Sakuma. “On strongly invertible knots”. In: *Algebraic and topological theories (Kinosaki, 1984)*. Kinokuniya, Tokyo, 1986, pp. 176–196.
- [26] M. Snape. “Homological invariants of strongly invertible knots”. PhD thesis. University of Glasgow, 2018.

- [27] J. Świątkowski. “On the isotopy of Legendrian knots”. In: *Ann. Global Anal. Geom.* 10.3 (1992), pp. 195–207. URL: <https://doi.org/10.1007/BF00136863>.
- [28] L. Watson. “Khovanov homology and the symmetry group of a knot”. In: *Advances in Mathematics* 313 (2017), pp. 915–946. URL: <https://doi.org/10.1016/j.aim.2017.04.003>.

DIPARTIMENTO DI MATEMATICA, LARGO BRUNO PONTECORVO 5, 56127 PISA, ITALY